PHYSICAL REVIEW A VOLUME 44, NUMBER 12 15 DECEMBER 1991

ARTICLES

Single effective neuron: Macroscopic potential and noise-induced bifurcations

A. R. Bulsara
Naval Ocean Systems Center, Materials Research Branch, San Diego, California 92152

W. C. Schieve
Physics Department, University of Texas, Austin, Texas 78712
and Center for Statistical Mechanics, University of Texas, Austin, Texas 78712

(Received 25 January 1991)

We consider a network of N symmetrically interconnected neutrons subject to additive as well as multiplicative (in the synaptic connections) noise. In a previous paper, the dynamics of a single neuron, in the presence of additive and multiplicative noise, was obtained through the procedure of adiabatic elimination. We analyze the macroscopic potential that describes the steady-state properties of this effective neuron, considering the effects of additive as well as multiplicative noise (in the synaptic connections).

PACS number(s): 05.40.+j, 87.10.+e, 05.45.+b

I. INTRODUCTION

In a previous paper [1] (hereafter referred to as I) the authors considered a network of N neutrons. Through the procedure of adiabatic elimination (separation of time scales) the dynamics of a single neuron interacting with the "bath" of N-1 neurons was obtained in closed form. This calculation reflects the recent upsurge of interest in single- (isolated) or few-neuron dynamics. This interest dates back to the work of Hopfield [2,3], who suggested a simple mathematical network that could reproduce a few of the collective properties of a biological neuron. It is precisely the relationship between the many-neuron connected model and a single-effective-neuron nonlinear dynamics that was explored in I. Other attempts along these lines include the work of Babcock and Westervelt [4], who examined simple models involving one or two nonlinear threshold switching elements which they modeled as Hopfield neurons. By introducing inertial terms in the dynamics they were able to demonstrate complicated bifurcation behavior including chaos. Their model of a single neuron with additive and multiplicative noise terms was considered by Bulsara, Ross, and Jacobs [5]. It was found that multiplicative noise (in the synaptic connection) would suppress the bistable character of the deterministic system as well as introduce bistability in the "thermodynamic potential" in parameter regimes where such behavior might not normally be expected. Li and Hopfield [6] have considered the neural proceedings in the olfactory bulb. They have found that the oscillatory activities in the bulb (as observed in electrophysiological experiments) may be modeled by a small group of coupled nonlinear oscillators. It is also worth pointing out that Skarda and Freeman [7] have evaluated electroencephalograph (EEG) data from the olfactory bulb. They find that many of their observations may be explained on the basis of simple "connectionist" models such as that of Hopfield.

In this work, we begin with the Fokker-Planck equation (or its equivalent stochastic differential equation) for the reduced probability density function of the single effective neuron. The steady-state solution of the Fokker-Planck equation may be expressed in terms of a macroscopic "potential" which determines how the physical observables of interest (i.e., moments of the relevant variable) behave at long times. The properties of this potential as a function of noise are examined in detail. In the remainder of this section, we briefly outline the adiabatic elimination procedure as it pertains to the derivation of the effective neuron dynamics. This is followed by an analysis of the turning points and bifurcation phenomena of the potential as a function of additive and multiplicative noise. In particular, we show that multiplicative noise (in the synaptic connections) may introduce new extrema in the potential as well as suppress extrema which would otherwise be present. In Sec. III we connect the results of this work with the studies of Ref. [5], in which these "noise-induced transitions" were considered for a single-neuron model having self-connections.

For simplicity, we will adopt the deterministic Hopfield model [2,3] of the form

$$C_i \frac{du_i}{dt} = \sum_{j \neq i = 1}^{N} J_{ij} \tanh u_j - \frac{u_i}{R_i} \ . \tag{1}$$

Here u_i is the potential of the ith neuron with input capacitance C_i and a leakage current due to the intermembrane resistance R_i. The interesting first term on the right-hand side of (1) represents the input to the soma from the other neurons with the characteristic saturation with potential of their firing rates, taken for simplicity to be a hyperbolic tangent function. We will take the neuron connectivity to be symmetric:

$$J_{ij}=J_{ji} \, , \qquad J_{ii}=0 \, . \tag{2}$$

It is important to point out that Eq. (1) is far more general than the specific application (associative memory) considered by Hopfield. In that case, the synaptic connectivities yield the number of patterns stored in the system via the Hebb rule. However, an equation of the form (1) has also been derived by Shamma [8] for the response of a single neuron in a mammalian auditory network, based on very simple nonlinear feedback circuit models. In this model, the coefficients represent the gain of the operational amplifiers and, depending on their sign, the nature of the excitation. It is precisely the properties of such a general, fully interconnected electronic network that we wish to consider in this work. Our work is, therefore, expected to shed some new light on the statistical mechanics of coupled oscillators of the form (1) with an electronic neural network taken to be the specific example, as has been done in I.

In I, we considered in detail the case of two connected neurons, and demonstrated how the results may be extended to three or more neurons. It is important to note that because of detailed balance considerations, the calculation for three or more neurons is markedly different from the two-neuron case, although the final effective single-neuron dynamics has the same form. These points have been considered in great detail in I and will not be repeated here. For simplicity, we will confine our discussion throughout this work to the case of two connected neurons subject to both additive and multiplicative Gaussian, δ-correlated noise. The two-neuron coupled stochastic differential equations may be written in the form

$$C_1\dot{U}_1=-\frac{u_1}{R_1}+[J+\delta J_2(t)]\tanh u_2+F(t) \, , \tag{3a}$$

$$C_2\dot{U}_2=-\frac{u_2}{R_2}+[J+\delta J_1(t)]\tanh u_1+F(T) \, . \tag{3b}$$

Here, we have allowed the connectivities to fluctuate:

$$J_{12}(t)=J+\delta J_2(t) \, , \qquad J_{21}(t)=J+\delta J_1(t) \, , \tag{4}$$

$$\langle \delta J_1(t)\delta J_2(0)\rangle=0 \, , \qquad \langle \delta J_1(t)\delta J_1(0)\rangle=\langle \delta J_2(t)\delta J_2(0)\rangle=\sigma^2\delta(t) \, , \tag{5}$$

$\delta(t)$ being the Dirac delta function. In addition, an additive (i.e., Langevin) white background current fluctuation $F(t)$ having zero mean and variance σ_a^2 and being uncorrelated with the multiplicative fluctuations is also assumed:

$$\langle F(t)\rangle=0=\langle F(t)\delta J_i(t)\rangle \, , \quad i=1,2 \qquad \langle F(t)F(0)\rangle=\sigma_a^2\delta(t) \, . \tag{6}$$

In the Ito interpretation [9] the corresponding two-dimensional Stratonovich-Fokker-Planck equation [9–11] for the probability density function $P\equiv P(u_1,u_2,t)$ is

$$\frac{\partial P}{\partial t}=-\frac{\partial}{\partial u_1}[A_1(u_1,u_2)P]-\frac{\partial}{\partial u_2}[A_2(u_1,u_2)P]+\tfrac{1}{2}B_1(u_2)\frac{\partial^2 P}{\partial u_1^2}+\tfrac{1}{2}B_2(u_1)\frac{\partial^2 P}{\partial u_2^2}+\frac{\sigma_a^2}{C_1C_2}\frac{\partial^2 P}{\partial u_1\partial u_2} \, , \tag{7}$$

with

$$A_1(u_1,u_2)\equiv-\frac{u_1}{R_1C_1}+\frac{J}{C_1}\tanh u_2 \, , \qquad A_2(u_1,u_2)\equiv-\frac{u_2}{R_2C_2}+\frac{J}{C_2}\tanh u_1 \, , \tag{8}$$

and

$$B_1(u_2)\equiv\frac{\sigma^2}{C_1^2}\tanh^2 u_2+\frac{\sigma_a^2}{C_1^2} \, , \qquad B_2(u_1)\equiv\frac{\sigma^2}{C_2^2}\tanh^2 u_1+\frac{\sigma_a^2}{C_2^2} \, . \tag{9}$$

We assume neuron 2 to be statistically rapidly varying and "slaved" by neuron 1 [12,13]. This may be achieved (see I) by taking $R_2\ll R_1$ and we may then write [1,12,13]

$$P(u_1,u_2,t)=h(2|1,t)g(1,t) \tag{10}$$

with

$$\int_{-\infty}^{\infty}h(2|1,t)du_2=1=\int_{-\infty}^{\infty}g(1,t)du_1 \, .$$

Here $h(2|1,t)\equiv h(u_2|u_1,t)$ is to be interpreted as a conditional probability density function to find u_2 given u_1. Substituting (10) into the original Fokker-Planck equation (7) one may obtain (the procedure is described in I) separate Fokker-Planck equations for h and g. In particular, we find for the probability density function of the "slow" or "stable" neuron

$$\frac{\partial}{\partial t}g(1,t)=-\frac{\partial}{\partial u_1}[F_1(u_1)g(1,t)]+\frac{1}{2}\frac{\partial^2}{\partial u_1^2}[D_1(u_1)g(1,t)] \, , \tag{11}$$

where, we introduce the quantities

$$F_1(u_1)\equiv-\frac{u_1}{R_1C_1}+\frac{J}{C_1}G(u_1) \, , \tag{12a}$$

$$D_1(u_1)\equiv C_1^{-2}[\sigma_a^2+\sigma^2H(u_1)] \, , \tag{12b}$$

$$G(u_1)\equiv\int_{-\infty}^{\infty}h(2|1)\tanh u_2\,du_2 \, . \tag{12c}$$

$$H(u_1)\equiv\int_{-\infty}^{\infty}h(2|1)\tanh^2 u_2\,du_2 \, . \tag{12d}$$

In the above integrals, $h(2|1)$ represents the long-time solution obtained from the corresponding Fokker-Planck equation [1] (the variable u_1 is treated as a constant when obtaining this solution, since u_2 relaxes on a far shorter time scale). This solution is readily seen to be a Gaussian in u_2 (assuming vanishing probability flux at the boundaries $u_2=\pm\infty$):

$$h(2|1)=K^{-1}\exp\left[\frac{2C_2^2}{\sigma^2\tanh^2 u_1+\sigma_a^2}\times\left[-\frac{u_2^2}{2R_2C_2}+\frac{Ju_2}{C_2}\tanh u_1\right]\right], \quad (13)$$

K being the normalization constant. The above solution is used in evaluating the integrals appearing on the right-hand side of (11), thereby reducing the latter to an effective one-neuron Fokker-Planck equation. In I, the integrals G and H have been evaluated by expanding the hyperbolic functions about the steady state $\bar{u}_2=JR_2\tanh u_1$. To order $(u_2-\bar{u}_2)^2$, this leads to

$$G(u_1)=\frac{b}{2a}\left[1-\frac{1}{2a}\right], \quad (14a)$$

$$H(u_1)=\left[\frac{b}{2a}\right]^2+\frac{1}{2a}\left[1-\frac{b^2}{2a^2}\right], \quad (14b)$$

where

$$a\equiv\frac{C_2/R_2}{\sigma^2\tanh^2 u_1+\sigma_a^2}, \quad b\equiv 2aJR_2\tanh u_1 .$$

In deriving the expressions (14a) and (14b) we have used the approximation $\tanh x\approx x$ for small x. Further, it has been assumed that the noise is moderate. Specifically, the assumptions

$$\sigma^2R_2\ll C_2, \quad \sigma_a^2R_2\ll C_2 \quad (15)$$

have been made. Together with the basic assumption $R_2\ll R_1$ (the backbone of the adiabatic elimination technique), these constitute the only constraints on the parameters throughout the remainder of the calculation. The adiabatic elimination technique effectively assumes that the "bath" is comprised of $N-1$ nonlinear oscillators that are actually only weakly nonlinear; in this regard, it makes contact with familiar mean-field-theoretical methods in statistical mechanics. The implications of such a procedure for the special case in which (1) represents a fully connected Hopfield model, used for instance as a content-addressable memory, are unclear; for the moment we simply reiterate that Eq. (1) is far more general and, in what follows, will be treated as a system of N coupled nonlinear oscillators, of which the associative network is a special case (depending, primarily, on the choices of the gain parameters). In I, the expressions (14a) and (14b) have been compared with the results obtained via numerical integration of (12c) and (12d). The agreement is impressive as long as the inequalities (15) are satisfied. We now consider the steady-state solutions of the single-neuron Fokker-Planck equation (11).

II. THE EFFECTIVE POTENTIAL

The long-time solution of the Fokker-Planck equation (11) may be written in the form [9,11,14]

$$g(u_1)=N^{-1}e^{-U(u_1)}, \quad (16)$$

N being the normalization constant and U the effective "potential" defined by

$$U(u_1)\equiv-2\int^{u_1}\frac{F_1(s)}{D_1(s)}ds+\ln D_1(u_1) . \quad (17)$$

Let us first consider the case of zero multiplicative noise. In this case, one readily obtains

$$U(u_1)=\frac{2C_1}{R_1\sigma_{1a}^2}\left[\frac{u_1^2}{2}-J^2R_1R_2\left[1-\frac{\sigma_{2a}^2R_2}{2C_2}\right]\times\ln(\cosh u_1)\right] . \quad (18)$$

In setting down this expression we have assumed that the additive noise strengths in the slow and fast neuron dynamics are not the same; one may derive Eq. (18) through a simple modification of the theory of the preceding section. For comparison purposes, it is instructive to write down the deterministic potential $U_d(u_1)$. This is the potential that corresponds to the case of no noise of any kind and may be obtained directly from Eq. (6) of I (setting $R_3=0$):

$$U_d(u_1)=(R_1C_1)^{-1}\left[\frac{u_1^2}{2}-J^2R_1R_2\ln(\cosh u_1)\right] . \quad (19)$$

It should be noted that the additional term in σ_{2a}^2 arises in (18) from the second term on the right-hand side of (14a). The adiabatic elimination technique introduces a noise-dependent renormalization of the drift term in the single-neuron dynamics. Hence, even though the diffusion term is constant in the limit of zero multiplicative noise, the structure of the potential is changed by this additional term in the drift.

The deterministic potential is bimodal above a critical value $\eta_c=1$ where $\eta\equiv J^2R_1R_2$. For the bimodal case, the minima of the potential occur at

$$u_1=\pm\left[1-\frac{1-\tanh^2\eta}{1-\eta\,\mathrm{sech}^2\eta}\right]\approx\eta\tanh\eta ,$$

the latter expression being true for large η. The potential has a maximum at $u_1=0$. The stochastic potential (18) is seen to have extrema at the same locations as the deterministic extrema in the limit of vanishingly small additive noise. However, in the presence of a finite amount of noise, the bifurcation point [defined here as the characteristic value η_c at which the potential (19) becomes bimodal] is a function of noise. Specifically, we must now define a bifurcation parameter $\eta_{sc}\equiv J^2R_1R_2(1-\sigma_{2a}^2R_2/2c_2)$ which controls the transition from unimodality to bimodality in the effective potential (19). It is interesting to note that the noise in the *fast* neuron dynamics changes the bifurcation behavior of the show or "effective" neuron dynamics; this is a consequence of the nonlinear character of the adiabatic elimination. For given values of J,R_1,R_2 such that the deterministic potential (19) is bimodal, the introduction of additive noise shifts the transition point for the onset of bimodality. Indeed, the noise causes the locations of the potential minima to change. One readily observes that for a critical noise strength

$$\sigma^2_{2ac}=\frac{2C_2}{R_2}\left[1-\frac{1}{J^2R_1R_2}\right], \qquad (20)$$

a potential which is bimodal in the absence of noise ($J^2R_1R_2>1$) will become monomodal. The above effect may be further quantified through a computation of the most probable value (defined by the condition $dU/du_1=0$, $d^2U/du_1^2>0$) as a function of the noise variance σ^2_{2a}. The most probable value displays a pitchfork bifurcation below the critical value σ^2_{2ac}. Above this value, the potential is a parabola centered at $u_1=0$ and the most probable value is zero. The above effects have been noted [15] in a mean-field description of an ensemble of linearly coupled nonlinear oscillators. Although noise-induced bifurcations in the macroscopic potential are quite common in the presence of multiplicative noise [5,16–18], they are not normally brought about by Langevin noise. However, the nonlinear nature of the transformations described in Sec. I and the subsequent renormalization of the drift term lead to the additive noise effectively postponing the onset of bistability in the single-neuron dynamics. Hence, our system does not violate Kurtz's theorem [19]. The effects discussed above are analogous to postponements induced by Langevin noise in swept-parameter nonlinear dynamic systems [20,21]. In these systems, the presence of the swept bifurcation parameter is a necessary condition for the transition to bimodality of the potential; the Langevin noise then delays or postpones the bifurcation. By contrast, in the problem at hand, the postponement occurs because of the separation of time scales in the coupled neuron system; this separation leads to the renormalization of the drift term in the single-neuron Fokker-Planck equation as described above. It should be noted that although the potential (18) becomes monomodal for $\sigma^2_{2a}>\sigma^2_{2ac}$ an accurate analytical description in this retime is not possible within the framework of our theory because of the constraints imposed by the inequality (15). In Fig. 1, we show the effective potential (18) for three different values of the additive noise variance σ^2. For the parameters of this figure one has $\sigma^2_{ac}\approx 10$. The destruction of bimodality with increasing noise is evident. Before going on, it is instructive to consider the case of very small multiplicative noise σ^2. In this case, the potential (18) may be written as

$$U(u_1)\approx\frac{2C_1}{R_1\sigma^2_{1a}}\left[\frac{u_1^2}{2}-J^2R_1R_2\left[1-(\sigma^2_{2a}+\sigma^2)\frac{R_2}{2C_2}\right]\times\ln(\cosh u_1)\right], \qquad (21)$$

with the critical additive noise variance now being given (for constant albeit small σ^2) by

$$\sigma^2_{2ac}\approx\frac{2C_2}{R_2}\left[1-\frac{1}{J^2R_1R_2}-\frac{\sigma^2R_2}{2C_2}\right].$$

The multiplicative noise *lowers* the threshold value σ^2_{2ac} from its value in the $\sigma^2=0$ case.

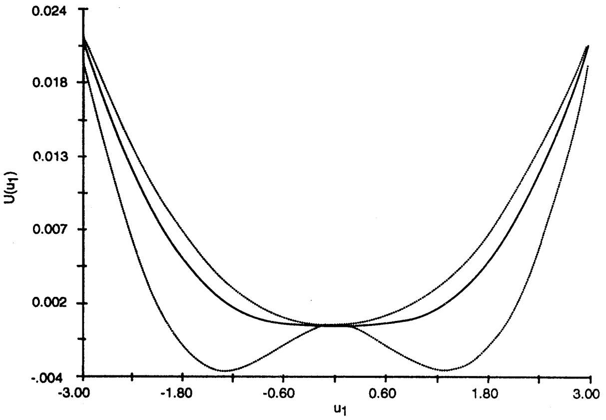

FIG. 1. Effective potential (18) for $(R_1,C_1,R_2,C_2,J)=(20,1,0.1,1,1)$ and $\sigma_a^2=5$ (bottom curve), 10 (middle curve–threshold case), and 15 (top curve).

We now turn to the case in which the multiplicative fluctuations are stronger, with variance σ^2. It is well known [16–18] that such fluctuations can qualitatively change the physical state of the system. As seen above, the Fokker-Planck equation for this case has a nonconstant diffusion term. By solving the Fokker-Planck equation in the steady state and computing the moments $\langle u_1^n(t)\rangle$ one obtains expressions for the physical observables in the system. At this point, two major differences between additive and multiplicative noise processes emerge. (1) The most probable value of a monomodal additive noise driven process in the steady state is simply the deterministic mean value, whereas the corresponding quantity for the multiplicative noise case depends on the noise strength. This means that the peaks of the long-time probability density function $g(u_1)$ no longer occur at the deterministic mean values; their location depends on σ^2. (2) For an additive noise process, global stability of the deterministic problem guarantees stability of the noise problem; this is no longer the case when multiplicative noise is introduced. The above comments constitute a general "rule of thumb" to distinguish between additive and multiplicative noise driven processes. Our system is, as seen in the preceding paragraph, an exception to the rule since additive noise can change the structure of the potential in a quantitative way for the case of coupled oscillators considered in this work.

We consider the potential (17) with F_1 and D_1 given by the expressions (12). Throughout the remainder of this work we assume that $\sigma_{1a}^2=\sigma_{2a}^2$, since our goal in what follows is to explore specifically the effects of finite multiplicative noise on the long-time neuron dynamics. In general, one cannot evaluate the potential U analytically for arbitrary σ^2. However, one may readily compute the "switching curve" whose zeros yield the extrema of the potential. This curve is obtained by setting $dU/du_1 \equiv f(u_1)=0$. One obtains, after some calculation,

$$f(u_1)\equiv u_1-J^2R_1R_2\left[1-\frac{\sigma_a^2R_2}{2C_2}-\frac{\sigma^2R_2}{2C_2}\right]\tanh u_1$$
$$+\left[\frac{\sigma^2R_1}{2C_1}\left[2J^2R_2^2-\frac{2J^2R_2^3\sigma_a^2}{C_2}+\frac{\sigma^2R_2}{C_2}\right]-\frac{J^2R_1R_2^2\sigma^2}{2C_2}\right]\tanh u_1\operatorname{sech}^2u_1-\frac{2J^2R_1R_2^3\sigma^4}{C_1C_2}\tanh^3u_1\operatorname{sech}^2u_1 \ . \qquad (22)$$

It is evident that the zeros of $f(u_1)$ will depend on the multiplicative noise variance σ^2, and for this case, on the additive noise variance σ_a^2 as well (although this is not generally the case, as noted above). The turning points of f may be found by setting $df/du_1=0=d^2f/du_1^2$. For the problem at hand, we can neglect the last term on the right-hand side of (22), recalling that R_2 is very small, by assumption. The calculation of the critical curves is then completely analogous to the calculation of Ref. [5], with the important difference that the coupling parameter J and the multiplicative noise variance σ^2 appear in the coefficients of $\tanh u_1$ as well as $\tanh u_1 \operatorname{sech}^2 u_1$ in contrast to the situation discussed in Ref. [5]. Following the procedure of Ref. [5], however, we may eliminate u_1 from (22) as well as the first and second derivatives of $f(u_1)$. We then obtain the pair of curves in the (J^2,σ^2) plane:

$$1-a_1J^2+b_1\sigma^2J^2+b_2\sigma^4=0 \qquad (23a)$$

and

$$A_1\sigma^8+A_2\sigma^6J^2+A_3\sigma^4J^2+A_4\sigma^2J^2$$
$$+A_5\sigma^4J^4+A_6\sigma^2J^4+A_7\sigma^4+A_8J^4=0 \ , \qquad (23b)$$

where

$$a_1=R_1R_2\left[1-\frac{\sigma_a^2R_2}{2C_2}\right], \quad a_2=\frac{R_1R_2^2}{2C_2} \ ,$$
$$b_1=\frac{R_1R_2^2}{C_1}\left[1-\frac{\sigma_a^2R_2}{C_2}\right], \quad b_2=\frac{R_1R_2}{2C_1C_2} \ ,$$
$$A_1=4b_2^2, \quad A_2=4b_2(2b_1-3a_2),$$
$$A_3=4a_1b_2, \quad A_4=12(a_2-b_1) \ ,$$
$$A_5=5a_2^2+4b_1^2-12a_2b_1 \ , \quad A_6=2a_1(2b_1-3a_2) \ ,$$
$$A_7=-12b_2, \quad A_8=a_1^2 \ .$$

Equations (23a) and (23b) define a pair of parabolas in the (J^2,σ^2) plane. They are plotted in Fig. 2 for two different values of the additive noise variance σ_a^2, the upper curve in each case corresponding to Eq. (23a).

We now discuss this phase diagram in detail. Much of our discussion will parallel the treatment of Ref. [5] since there are striking similarities between the two systems (the work of Ref. [5] pertains to a single electronic Hopfield-like element in a neural circuit, having a nonzero fluctuating self-coupling term and negligible coupling to other neurons). There are also some marked dissimilarities. These will be explored briefly in the remainder of this section and more fully in Sec. III. We first note that unlike the phase diagram of Ref. [5], changing the additive noise variance σ_a^2 results in a shift of the curves described by (23). This is evident upon an examination of Fig. 2. In particular, one observed that the point of intersection of the upper curve with the vertical axis is displaced upward with increasing σ_a^2. Since this point represents the value of J^2 at which the potential changes from monomodal (below this point) to bimodal (above this point) in the absence of multiplicative noise, the observes shift is merely a manifestation of the effects described at the beginning of this section: additive noise can change the number of peaks in the probability density function in this case, even in the absence of multiplicative noise. We note in passing that for the case of a general assembly of coupled nonlinear oscillators described by (1), the parameter J can take on any value [J is related to the gain parameter of the nonlinear element in a single elemental circuit contained in (1)]; for the special case of an associative memory, the allowed J values are restricted by the Hebb rule which determines the number of stored configurations. It is important to note [as is evident from an examination of (22) and (23)] that the critical dynamics of the network involve the product J^2R_1 in

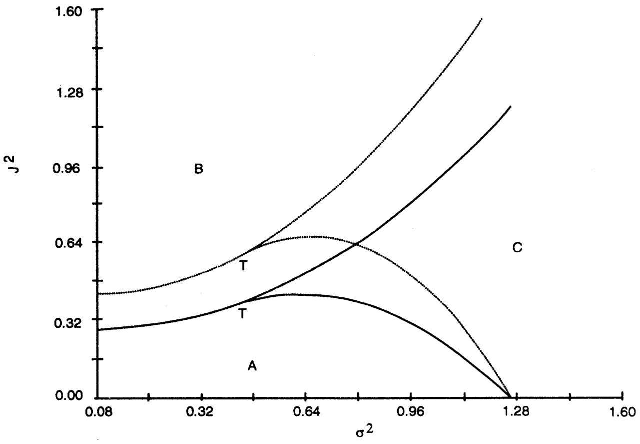

FIG. 2. Multiplicative noise: critical curves defined by (23a) and (23b) for $\sigma_a^2=1$ (solid curve) and 10 (dotted curve). $(R_1,C_1,R_2,C_2,J)=(50,1,0.075,1,1)$.

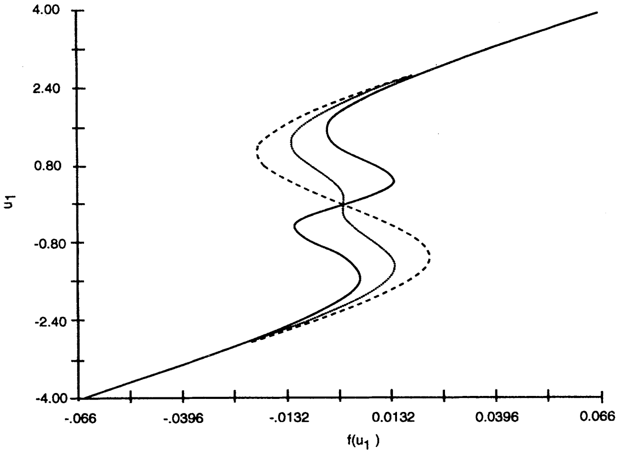

FIG. 3. Switching curves (22) for $J=0.8$, $\sigma_a^2=1$ and $\sigma^2=0.5$ (dashed curve), 0.8 (dotted curve–threshold case), and 1.1 (solid curve). Other parameters as in Fig. 2.

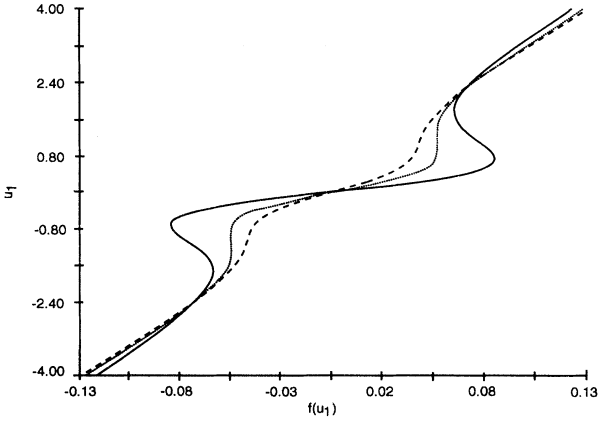

FIG. 5. Switching curves for $\sigma_a^2=1$, $J=0.4$ and $\sigma_m^2=0.96$ (dashed curve), 1.16 (dotted curve–threshold case) and 1.6 (solid curve). Other parameters as in Fig. 2. Other parameters as in Fig. 1.

all the terms. Hence, one may also achieve the bifurcation phenomena described in this section by keeping J fixed and varying the resistance R_1 of the slow neuron (making sure that the basic conditions of Sec. I are always met).

The phase diagram may be divided naturally into three regions. In region A, the potential is always monomodal. This region encompasses a small set of values of J for which the potential would be expected to be bimodal in the absence of multiplicative noise. One sees, therefore, a suppression of the bimodality of the multiplicative noise. In region B, the coupling parameter J dominates the structure of the potential. As one passes from region A to region B the switching curve passes through a point of inflexion and develops two stable branches, (i.e.), Eq. (22) has three real roots. The potential U which is monomodal in region becomes bimodal in region B, having a maximum at $u_1=0$. This is also the location of the point of inflexion on the switching curve for the critical case in which the parameters J and σ^2 are taken to correspond to the point T. The coordinates of this critical point, referred to in Refs. [5] and [18] as a noise-induced triple point, may be found by solving the simultaneous equations

$$a_1J^2-a_2J^2\sigma^2=\tfrac{4}{3}\ , \qquad (b_1-a_2)J^2\sigma^2+b_2\sigma^4=\tfrac{1}{3}\ . \tag{24}$$

The effects of crossing the critical curve from region B to region C are demonstrated in Fig. 3, in which we plot the switching curves corresponding to values of (J^2,σ^2) in region B, on the critical curve, and in region C. The potentials corresponding to these cases are shown in Fig. 4. One observes that a point of inflexion develops on the switching curve (at $u_1=0$) and, upon crossing into region C, that Eq. (22) has an additional real zero; an additional minimum develops in the potential at $u_1=0$. Region C corresponds to the region in which multiplicative fluctuations play a significant, perhaps dominant role in the behavior of the effective potential. In Ref. [5], it was seen that in general one observes additional minima in the potential, and in region C only for certain values of an external symmetry-breaking constant (i.e., dc) driving term. A similar effect is observed in this case. As an example of this behavior we plot in Fig. 5 the switching curves corresponding to three values of σ^2 in the regions $A-C$. It is evident that for the most part, the curves admit of only one zero. However, for certain appropriately chosen values of an external constant driving term Eq. (22) would indeed have three zeros. This point has been treated in great detail in Ref. [5] and will not be discussed further. It is important to note, in concluding this section, that the potentials calculated in this section are obtained via the approximation (14), with the noise variance always selected so that (15) is satisfied. The curves of Fig. 4 differ very slightly from the "exact" potential which would be obtained via numerical integration in (12c) and

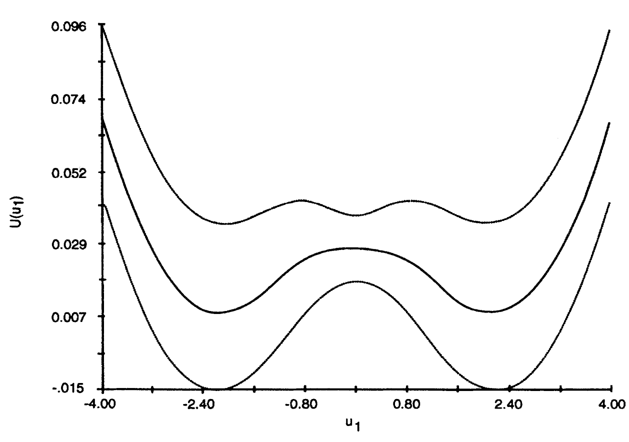

FIG. 4. Potential $g(u_1)$ corresponding to the cases of Fig. 3: $\sigma^2=1.1$ (top curve), 0.8 (middle curve), and 0.5 (bottom curve).

(12d). In particular, the approximation used here yields the correct turning points and extremum behavior of the potential for the parameter ranges considered in this work.

III. CONNECTION WITH OTHER WORK: THE CASE OF *A PRIORI* SELF-COUPLING

Throughout this work we have assumed that self-coupling terms involving the coefficients J_{ii} in (2) are zero *a priori.* However, as has been shown in I, a purely deterministic treatment of the N-neuron problem results in an expression for an "effective" self-coupling term $J_{11}\tanh u_1$ after the adiabatic elimination is carried out. Our treatment of Ref. 5 concerned the case when this self-coupling term was present *a priori* in the stochastic problem of a single Hopfield-like computation element and, moreover, was much greater than the cross-coupling terms. In fact, in this treatment, the neuron was effectively isolated. As discussed in the preceding section many of the effects of multiplicative noise observed in the system of Ref. [5] are duplicated in the problem at hand, although there are several important differences (notably the effects of purely additive noise). In what follows we derive, in a self-consistent manner, the single-effective-neuron dynamics for the case when self-coupling terms are included at the outset, namely, we consider the fact that J_{ii} is nonvanishing. Once again, we consider the case of two coupled neurons, one of which (the "fast" neuron) evolves to its steady state on a much faster time scale. Our treatment follows that of I but several important differences will emerge. Ultimately, we show that this treatment leads, under certain conditions, to the results of Ref. [5].

In the presence of self-coupling effects, the terms $J_{11}\tanh u_1$ and $J_{22}\tanh u_2$ are added to the right-hand sides of Eqs. (3a) and (3b), respectively. We further assume that Gaussian δ-correlated fluctuations are present in the self-coupling:

$$\begin{aligned} J_{11} &= J_s + \delta J_{11} \ , \\ J_{22} &= J_s + \delta J_{22} \ , \\ \langle \delta J_{ii} \rangle &= 0, \quad \langle \delta J_{ii}(t)\delta J_{ii}(t-\tau)\rangle = \sigma_{si}\delta(\tau), \quad i=1,2 \ . \end{aligned} \tag{25}$$

It is also assumed that there are no cross correlations between δJ_{ii} and δJ_k occurring in (3) or with the Langevin noise $F(t)$ (we assume the same additive noise variance σ_a^2 in the slow and fast neuron dynamics). Proceeding as in I we construct the Fokker-Plance equation for the probability density function $P(u_1,u_2,t)$:

$$\begin{aligned} \frac{\partial P}{\partial t} = &-\frac{\partial}{\partial u_1}[q_1(u_1,u_2)P] - \frac{\partial}{\partial u_2}[q_2(u_1,u_2)P] \\ &+\frac{1}{2}\frac{\partial^2}{\partial u_1^2}[Q_1(u_1,u_2)P] + \frac{1}{2}\frac{\partial^2}{\partial u_2^2}[Q_2(u_1,u_2)P \\ &+\frac{\sigma_a^2}{C_1C_2}\frac{\partial^2 P}{\partial u_1 \partial u_2} \ , \end{aligned} \tag{26}$$

where we define the quantities

$$\begin{aligned} q_1 = &-\frac{u_1}{R_1c_1} + C_1^{-1}(J_s\tanh u_1 + J\tanh u_2) \\ &+\tfrac{1}{2}C_1^{-2}\sigma_{s1}^2\tanh u_1 \operatorname{sech}^2 u_1 \\ q_2 = &-\frac{u_2}{R_2C_2} + C_2^{-1}(J_s\tanh u_2 + J\tanh u_1) \\ &+\tfrac{1}{2}C_2^{-2}\sigma_{s2}^2\tanh u_2 \operatorname{sech} u_2 \\ Q_1 = &\ C_1^{-2}(\sigma^2\tanh^2 u_2 + \sigma_{s1}^2\tanh^2 u_1 + \sigma_a^2) \ , \\ Q_2 = &\ C_2^{-2}(\sigma^2 \mathrm{tahn}^2 u_1 + \sigma_{s2}^2\tanh^2 u_2 + \sigma_a^2) \ . \end{aligned} \tag{27}$$

We now assume that the joint probability density function P may be factored as

$$P(u_1,u_2,t) \equiv h_s(2|1,t)g_s(1,t) \tag{28}$$

with h_s and g_s being separately normalized to unity. We then obtain separate Fokker-Planck equations for the density functions h_s and g_s:

$$\frac{\partial h_s}{\partial t} = -\frac{\partial}{\partial u_2}(q_2h_s) + \frac{1}{2}\frac{\partial^2}{\partial u_2^2}(Q_2h_s) \ , \tag{29}$$

and

$$\frac{\partial g_s}{\partial t} = -\frac{\partial}{\partial u_1}[A(u_1)g_s] + \frac{1}{2}\frac{\partial^2}{\partial u_1^2}[B(u_1)g_s] \ . \tag{30}$$

Equation (29) must be solved in the steady state, treating u_1 as a constant. A solution may be formally set down in the form (17), however, the integral occurring in the solution cannot be evaluated analytically. If such a solution were available, however, it would be used to compute the drift and diffusion expressions in (30). These expressions are

$$A(u_1) = \int q_1(u_1,u_2)h_s(2|1)du_2 \tag{31a}$$

which may be cast in the form

$$\begin{aligned} A(u_1) = &-\frac{u_1}{R_1C_1} + J_s\tanh u_1 + \frac{\sigma_{s1}^2}{2C_1^2}\tanh u_1 \operatorname{sech}^2 u_1 \\ &+\frac{J}{C_1}\int \tanh u_2 h_s(2|1)du_2 \ , \end{aligned} \tag{31b}$$

and

$$B(u_1) = \int q_1(u_1,u_2)h_s(2|1)du_2 \tag{32a}$$

which may be cast in the form

$$\begin{aligned} B(u_1) = &\ C_1^{-2}(\sigma_{s1}^2\tanh^2 u_1 + \sigma_a^2) \\ &+\sigma^2C_1^{-2}\int \tanh^2 u_2 h_s(2|1)du_2 \ . \end{aligned} \tag{32b}$$

Rather than evaluate the solution $h_s(2|1)$ in general, we consider the special case

$$\frac{\sigma_{s2}^2}{\sigma_a^2} \ll 1, \quad \frac{\sigma_{s2}^2R_2}{C_2} \ll 1 \ .$$

These conditions are tantamount to assuming that the fluctuations in the self-coupling term of the fast neuron are small; the second condition follows naturally as a consequence of this condition and the conditions $R_2 \ll R_1$ for adiabatic elimination. Under these conditions, we may set down, after some calculation, a steady-state solution for $h_s(2|1)$:

$$\begin{aligned} h_s(2|1) &= N^{-1}(u_1)e^{-U_s} , \\ U_s &\equiv \frac{2C_2/R_2}{\sigma_a^2+\sigma^2\tanh^2 u_1}\left[\frac{u_2^2}{2} - J_s R_2 \ln(\cosh u_2) \right. \\ &\qquad \left. - J R_2 u_2 \tanh u_1 \right] , \end{aligned} \tag{33}$$

$N(u_1)$ being the normalization (with respect to u_2). This solution is seen to differ from (13) in the presence of the self-coupling term in the exponential. We may now evaluate the integrals occurring on the right-hand sides of (31) and (32). If in addition to the assumption of small σ_{s2}^2, we assume that the cross-coupling terms are small ($J \ll J_s$ and $\sigma^2 \ll \sigma_{1s}^2$), we can show (this has been carried out numerically) that the terms containing the integrals on the right-hand sides of (31b) and (32b) are negligible compared to the remaining terms in these expressions. We then obtain the steady-state solution for the effective neuron in the form

$$g_s(u_1) \equiv K^{-1}\exp[-\Phi(u_1)] \tag{34}$$

with the potential Φ given by an expression of the form (17):

$$\Phi(u_1) = -2\int^{u_1}\frac{A(s)}{B(s)}ds + \ln B(u_1) .$$

In light of the preceding analysis, the drift and diffusion terms are now given by

$$A(u_1) = -\frac{u_1}{R_1C_1} + \frac{J_s}{C_1}\tanh u_1 + \frac{\sigma_{s1}^2}{2C_1^2}\tanh u_1 \operatorname{sech}^2 u_1 \tag{35a}$$

and

$$B(u_1) = C_1^{-2}(\sigma_{s1}^2\tanh^2 u_1 + \sigma_a^2) . \tag{35b}$$

This is *precisely* the potential of Ref. [5]. We thus see that our previously considered model of a single isolated neuron with self-coupling (derived from a feedback loop in the electronics) may be obtained in a consistent manner, via the adiabatic elimination procedure, from an N-neuron network.

IV. DISCUSSION

In this work, we have extended our earlier calculations [1] to include an analysis of the long-time behavior of the probability density function that describes a single effective neuron. The effective neuron dynamics were derived in I by assuming it to be adiabatically coupled to a "bath" of neurons which may be treated as being in their steady states. Although we have considered the case for just two coupled neurons in this work, the treatment of I should make it evident that the results may be carried over to the N-neuron case. Both additive and multiplicative noise effects have been considered. An interesting result is the suppression of the transition to bimodality in the potential, induced by Langevin noise. The result, which would not occur in the case of a single isolated oscillator (e.g., the single isolated element of Ref. [5]) is similar to an observation by Shiino [15] on a network of coupled bistable oscillators described by a mean-field theory. The central result of Ref. [15] is that such systems of many coupled nonlinear oscillators may exhibit mean-field-type phase transitions, and the critical behavior may be explored via the reduced Fokker-Planck equation describing the dynamics of a single oscillator. Strictly speaking, the term "phase transition" applies to a qualitative change in the physical observable (usually the most probable value) as well as changes in the shape of the many-body probability density function. Further, the term generally applies only in the "thermodynamic limit" of a large number of oscillators. In this context, it seems reasonable to ask the question of what does one mean, in a practical situation, by a larger number of oscillators? Certainly we have seen in this work that two coupled nonlinear oscillators may exhibit the effects described in Ref. [15]. The theory developed in I indicates that our results would be qualitatively similar if we considered the N-neuron problem (although the calculation is likely to be overly tedious). Since the effect of Langevin noise is to modify the shape of the potential through modification of the nonlinearity η defined by (19) (we are, in fact led to define an additional bifurcation parameter η_{sc} in the presence of Langevin noise), it seems reasonable to assume that the Langevin noise does in fact introduce a pitchfork bifurcation in the long-time dynamics of u_1; this bifurcation is observed in the most probable value of u_1 above the critical η_{sc}, an effect also observed in Ref. [15]. It is of interest to note that the effects of the Langevin noise are similar to those that result from multiplicative fluctuations with one important difference: the Langevin noise may shift the transition point (from unimodality to bimodality) in the effective single-neuron potential, but it cannot introduce additional minima (of the kind observed in Fig. 4, for example) in the potential. We have seen that the effects of Langevin noise alone manifest themselves through an additional u_1-dependent term in the drift F_1 appearing in the potential (17). However, the diffusion term D_1 remains a constant, unlike the case when multiplicative fluctuations ($\sigma^2 > 0$) are included.

Multiplicative noise (which enters the system through fluctuations in the cross-coupling terms) also alters the structure of the potential. Specifically, the multiplicative noise can postpone or advance the onset of bimodality. In some cases (exemplified in Figs. 3 and 4), the multiplicative noise may actually introduce additional wells in the potential. In other regimes (region C of Fig. 2) the multiplicative noise introduces bimodality only for certain values of the system and noise parameters (as discussed in Ref. [5], the transitions in this regime take place for certain well-defined values of an external symmetry-breaking dc term). The stationary probability density $g(u_1)$ permits us to obtain all the moments $\langle u_1^n \rangle$

of the system. In practice these constitute the physical observables, although it has been demonstrated [22] that the stationary probability density is itself an experimental observable. Before leaving this subject, it is instructive to compare the results of Sec. II with our earlier work [5] on the stochastic generalization of the simple single-neuron model with self-coupling terms only. At first glance it might appear that the effects of multiplicative noise (exemplified in Figs. 3–5) are qualitatively similar to those encountered in Ref. [5]. However, there exist several quantitative differences between the two theories. Perhaps the most striking dissimilarity is the role played by the Langevin noise in the system considered in this work. We have seen that in the presence of additive as well as multiplicative noise, the phase diagram of Fig. 2 is actually displaced by changes in the variance σ_a^2 of the Langevin noise; the noise plays the role of a symmetry-breaking "order parameter" with the noise-induced triple point T being a function of σ_a^2. As described above, this is a consequence of the nonlinear character of the adiabatic elimination procedure which forms the basis of this work. No such effects occur in the method of Ref. [5]; the effects of Langevin noise in that case are to simply alter the width of the probability density function. The above effects may be observed in the equations governing the switching curves in Figs. 3 and 5. The coefficients multiplying the hyperbolic functions in (22) are functions of both the cross-coupling strength J as well as the multiplicative and additive noise variances. This leads to the somewhat complicated equations (23a) and (23b) describing the phase diagram (Fig. 2). The situation is markedly simpler in Ref. [5] in which the coefficient of $\tanh u_1$ involves only the nonlinearity parameter and the coefficient of $\tanh u_1 \operatorname{sech}^2 u_1$ involves only the multiplicative noise variance. The switching curve in Ref. [5] does not depend at all on the additive noise variance, unlike the situation encountered in this work.

It is important to point out that we have not addressed the dynamical evolution of the probability density function. It is well known that in the neighborhood of a critical point one observes "critical slowing down," i.e., the system responds on a time scale that becomes progressively larger as one approaches the critical point. Such behavior has indeed been observed near a noise-induced critical point in some exactly solvable model systems [16]. The study of such behavior typically focuses on a computation [9,14] of the first eigenvalue λ_1 of the Fokker-Planck equation. This eigenvalue describes the long-time behavior of the system and may be identified with a "switching rate," i.e., the rate at which the system undergoes transitions between the most probable states (characterized by the peaks of the probability density function). For the system at hand, if λ_1 is small and the time scale ($\approx \lambda_1^{-1}$) on which one observes noise-induced transitions is much greater than the time scale that describes hysteresis, then the additional noise-induced steady states are indeed physical, manifesting themselves as multivaluedness in the mean value $\langle u_1(t) \rangle$. A detailed consideration of these issues is beyond the scope of this paper.

Finally, we have shown that the simple model of a single Hopfield-like electronic element that formed the basis of our earlier work [5] is indeed consistent with the results of this work. Specifically we see that starting with the N-body Hopfield model (in which *ab initio* self-coupling terms are included) we may obtain, in a self-consistent manner, precisely the potential that was discussed in Ref. [5]. Both Langevin as well as multiplicative fluctuations have been included and it has been assumed that the cross-coupling terms are very weak. Moreover, it is assumed that the fluctuations in the self-coupling terms (arising from the feedback) are negligible in the "fast" neurons. This assumption is reasonable since these neurons are assumed to have attained their steady-state values on a faster time scale than the "slow" neuron; this assumption is the basis of the slaving principle.

ACKNOWLEDGMENTS

A.R.B. acknowledges useful conversations with Dr. J. C. Hicks (Naval Ocean Systems Center) and Dr. Frank Moss (Physics Department, University of Missouri, St. Louis). This work was supported, in part, by the Office of Naval Research under Grant No. N00014-90-AF-00001.

---

[1] W. Schieve, A. Bulsara, and G. Davis, Phys. Rev. A **43**, 2613 (1991).
[2] J. Hopfield, Proc. Natl. Acad. Sci. **79**, 2554 (1982).
[3] J. Hopfield, Proc. Nat. Acad. Sci. **81**, 3088 (1984).
[4] K. Babcock, and R. Westervelt, Physica D **28**, 305 (1987).
[5] A. Bulsara, R. Boss, and E. Jacobs, Biol. Cyber. **61**, 211 (1989).
[6] Z. Li and J. Hopfield, Biol. Cyber. **61**, 379 (1989).
[7] C. Skarda and W. Freeman, Behav. Brain Sci. **10**, 161 (1987).
[8] S. Shamma, in *Methods of Neuronal Modelling,* edited by C. Koch and I. Segev (MIT, Cambridge, MA, 1989).
[9] C. Gardiner, *Handbook of Stochastic Methods* (Springer-Verlag, Berlin, 1985), Chap. 6.
[10] R. Stratonovich, in *Noise in Nonlinear Dynamical Systems,* edited by F. Moss and P. McClintock (Cambridge University Press, London, 1989), Vol. 1.
[11] R. Stratonovich, *Topics in the Theory of Random Noise* (Gordon and Breach, New York, 1963), Vol. 1.
[12] H. Haken, *Synergetics* (Springer-Verlag, Berlin, 1977).
[13] H. Haken, *Advanced Synergetics* (Springer-Verlag, Berlin, 1983).
[14] H. Risken, *The Fokker Planck Equation* (Springer-Verlag, Berlin, 1984).
[15] M. Shiino, Phys. Rev. A **36**, 2393 (1987).
[16] W. Horsthemke and R. Lefever, *Noise-Induced Transitions* (Springer-Verlag, Berlin, 1984).
[17] A. Bulsara, W. Schieve, and R. Gragg, Phys. Lett. **A68**, 294 (1978).
[18] A. Bulsara, W. Schieve, and E. Jacobs, Physica **146A**, 126

(1987).
[19] T. Kurtz, J. Chem. Phys. **50**, 460 (1969).
[20] B. Morris and F. Moss, Phys. Lett. **118**, 117 (1986).
[21] R. Manella, P. McClintock, and F. Moss, Phys. Lett. **120**, 11 (1987).
[22] F. Moss and P. McClintock, in *Fluctuations and Sensitivity in Nonequilibrium Systems,* edited by W. Horsthemke and D. Kondepudi (Springer, Berlin, 1984).